A computer simulation approach to quantify the *true* area and *true* area compressibility modulus of biological membranes

Enrique Chacón,[1,a)] Pedro Tarazona,[2,b)] and Fernando Bresme[3,c)]
[1]*Instituto de Ciencia de Materiales de Madrid, CSIC, 28049 Madrid, Spain and Instituto de Ciencia de Materiales Nicolás Cabrera, Universidad Autónoma de Madrid, Madrid 28049, Spain*
[2]*Departamento de Física Teórica de la Materia Condensada, Condensed Matter Physics Center (IFIMAC), and Instituto de Ciencia de Materiales Nicolás Cabrera, Universidad Autónoma de Madrid, Madrid 28049, Spain*
[3]*Department of Chemistry, Imperial College London, SW7 2AZ London, United Kingdom*

(Received 27 March 2015; accepted 6 July 2015; published online XX XX XXXX)

We present a new computational approach to quantify the area per lipid and the area compressibility modulus of biological membranes. Our method relies on the analysis of the membrane fluctuations using our recently introduced coupled undulatory (CU) mode [Tarazona *et al.*, J. Chem. Phys. **139**, 094902 (2013)], which provides excellent estimates of the bending modulus of model membranes. Unlike the projected area, widely used in computer simulations of membranes, the CU area is thermodynamically consistent. This new area definition makes it possible to accurately estimate the area of the undulating bilayer, and the area per lipid, by excluding any contributions related to the phospholipid protrusions. We find that the area per phospholipid and the area compressibility modulus features a negligible dependence with system size, making possible their computation using truly small bilayers, involving a few hundred lipids. The area compressibility modulus obtained from the analysis of the CU area fluctuations is fully consistent with the Hooke's law route. Unlike existing methods, our approach relies on a single simulation, and no *a priori* knowledge of the bending modulus is required. We illustrate our method by analyzing 1-palmitoyl-2-oleoyl-sn-glycero-3-phosphocholine bilayers using the coarse grained MARTINI force-field. The area per lipid and area compressibility modulus obtained with our method and the MARTINI forcefield are consistent with previous studies of these bilayers. © *2015 AIP Publishing LLC.* [http://dx.doi.org/10.1063/1.4926938]

I. INTRODUCTION

Lipid bilayers are one of the main structural constituents of biological membranes. The elastic properties of bilayers play a key role in determining the anchoring, insertion and function of trans-membrane proteins,[1] and ~~possibly~~ influence protein signal transduction.[2,3] The elastic properties further ~~influence~~ the mesoscopic curvature of the membranes, and hence play a key role in the formation of vesicles as well as bilayer fusion.[4] One of the relevant elastic properties of bilayers is the area compressibility modulus, K, which is directly proportional to the bilayer area fluctuations $\langle A^2\rangle - \langle A\rangle^2$. Simulation ~~works~~ reported over the last two decades have quantified the area compressibility moduli and the bilayer area fluctuations. A major difficulty in the analysis of existing results is the lack of a unique definition of the true area of a tensionless membrane. The bilayer fluctuations ~~are often~~ interpreted as a combination of undulatory and peristaltic modes.[5–8] The Helfrich hamiltonian[9] provides a good description of the collective bilayer long-wavelength undulatory modes. However, for short wavelength modes involving large wavevectors (q), the undulatory fluctuations of the two phospholipid layers become uncorrelated, due to the so called peristaltic fluctuations, which involve local changes of the membrane width, as well as to protrusions of single lipids.[10] It has been shown that the undulatory mode features a crossover between *coupled undulatory* fluctuations, in which the bilayer fluctuates as a whole, and the *uncoupled undulatory* independent fluctuations of each layer. The true area of a bilayer is determined by the coupled mode; however, this mode is difficult to isolate, since there is a smooth transition between the coupled and uncoupled regime, which results in the mixing of ~~the~~se modes, making difficult the evaluation of the true area. Our work focuses on the definition of a new mode that circumvents this problem by eliminating the inclusion of high wave number modes that should not contribute to the true area of the bilayer.

The difficulties associated to the analysis of the membrane fluctuations have resulted in other problems. One of the most important is the dependence of the compressibility modulus with the surface tension,[4] which has not yet been fully resolved. We will show later that our approach allows us to resolve this problem too.

The lack of a common approach to compute the true area and the area compressibility modulus has prompted the development of different approaches. The simplest choice is the computation of the cross sectional area of the bilayer, $A^{\parallel}$, whose mean value $A_{\parallel} \equiv \langle A^{\parallel}\rangle$ and fluctuations $\langle A^{\parallel 2}\rangle - A_{\parallel}^2$ may be easily obtained. However, for free membranes (zero surface

a)Electronic address: echacon@icmm.csic.es
b)Electronic address: pedro.tarazona@uam.es
c)Electronic address: f.bresme@imperial.ac.uk

tension), $A_\parallel$ is not an extensive thermodynamic variable, i.e., it is not proportional to the number of phospholipid molecules per layer $N_{\rm Phos}$. In fact, the mean projected area per phospholipid, $a_\parallel \equiv \langle A^\parallel \rangle / N_{\rm Phos}$, and the corresponding area compressibility, $K^\parallel$, depend on the size of the simulated membrane.[8,11] Helfrich's theory[9,12,13] provides a theoretical route to understand this size dependence. The analysis of the size dependence of $\langle a_\parallel \rangle$ and $K^\parallel$ provides in turn a route to obtain the true area per lipid, $\langle a \rangle$, and the true compressibility, K. Although the Helfrich theory is formally well defined, the numerical procedure to calculate the relevant equations (see the Eqs. 19 and 20 in Ref. 12) can lead to different results. Its implementation requires the introduction of an *ad hoc* cutoff to separate the undulatory and protrusion modes, but there is no general agreement on the value that should be employed for the cutoff. Waheed and Edholm[12] chose as cutoff $2\pi/\sqrt{\langle a_\parallel \rangle}$, while Lindhal and Edholm[7] used $2\pi/d$, where d is the mean membrane thickness. Different cutoffs result in different compressibility moduli, hence adding uncertainty to the computation of this property. From a more practical point of view, the Helfrich approach requires computations involving bilayers with different sizes, hence increasing the computational cost of the method.

Following the discussion above, it is clear that an accurate definition of the true membrane area and its area compressibility modulus is still lacking. It would appear that the best candidate to compute the true area is the area of the undulatory surface, $A^{\rm U}$, which is defined by the arithmetic mean for the positions of the two bilayer leaflets.[7,8] However, $A^{\rm U}$ includes contributions from the uncorrelated molecular protrusions in each leaflet (see Fig. 1-left), which should not be included in the evaluation of the true area. As an alternative, we propose to use the area of the peristaltic surface $A^{\rm P}$, see Fig. 1-right, to eliminate the protrusion contribution to $A^{\rm U}$ and to define the *coupled undulatory* area,

$$A^{\rm CU} = A^{\rm U} - (A^{\rm P} - A^\parallel) \equiv A^{\rm U} - \Delta A^{\rm P}. \qquad (1)$$

We will show that this area provides a robust approach to quantify, using computer simulations, the true area of biological membranes. This approach is based on our recent analysis of the spectrum of elastic deformations in a bilayer membrane.[14]

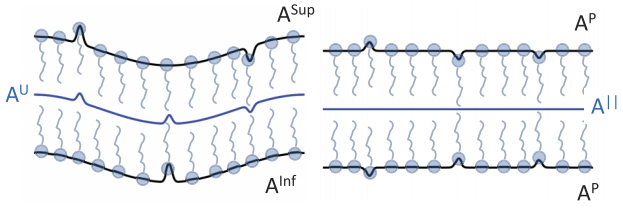

FIG. 1. (Left) The area $A^{\rm U}$ of the bilayer calculated from the plane corresponding to the arithmetic mean of the two bilayer leaflets (sup and inf). This surface contains contributions from the uncorrelated molecular protrusions (see spikes) in each leaflet. (Right) Representation of the membrane featuring two symmetric peristaltic (P) modes in each leaflet, constructed to keep the local thickness as in the real (left) membrane. The collective undulations of the membrane do not contribute to the area $A^{\rm P}$, but the molecular protrusions give equal contribution to $A^{\rm P}$ and $A^{\rm U}$. We propose that the difference $A^{\rm CU} \equiv A^{\rm U} - (A^{\rm P} - A^\parallel)$ is a good measure of the true area of the membrane. A detailed explanation of definitions introduced in this figure is given at the end of Section III.

The Fourier analysis of $A^{\rm U}$ and $A^{\rm CU}$ shows that Eq. (1) allows a rigorous separation of the molecular protrusion from the undulatory modes. The evaluation of $A^{\rm CU}$ does not require the use of any *ad-hoc* wavevector cutoff, and it may be obtained directly from, e.g., the area of the U and P triangulated surfaces. Hence, our approach circumvents current problems associated to the use of cutoffs to separate fluctuation modes, allowing the determination of the true area. We will show that $A^{\rm CU}$ complies with the properties of an extensive property and features a rapid time relaxation, sub-nanosecond timescales, towards its mean equilibrium value $A_{\rm CU} = \langle A^{\rm CU} \rangle$.

The paper is structured as follows. First, we provide details on the model bilayers and simulation approaches employed in this work. A discussion of the membrane fluctuations in terms of the coupled undulatory (CU) and peristaltic modes is provided, followed by a detailed description of the new coupled-undulatory area, $A_{\rm CU}$. We then report our result for the membrane area and area compressibility modulus as a function of the membrane cross sectional area and membrane tension. A final section containing the most relevant conclusions closes the paper.

II. MODEL AND SIMULATION DETAILS

We have performed simulations of POPC (1-palmitoyl-2-oleoyl-sn-glycero-3-phosphocholine) bilayers, which is a major component of many biological membranes. We use the MARTINI coarse-grained model, where the phospholipid is modeled as a collection of beads joined by bonding and angular terms.[15] The MARTINI model reproduces quantitatively a number of relevant properties, such as the bending modulus.[14] Also it can be used to model multicomponent bilayers, e.g., those containing cholesterol, hence enabling the prediction of complex multicomponent phase diagrams.[16]

All our simulations were performed at 320 K. At this temperature, POPC is in the L_d phase. We truncated and shifted the Lennard-Jones non-bonding short range interactions at 0.9 nm. A shifted coulomb potential with a 1.2 nm cutoff and an effective dielectric constant of 15 were used to model the electrostatic interactions arising from the charges in the POPC head groups.

The bilayers consisted of $N_{\rm Phos}$ phospholipids per layer and $N_{\rm Water}$ coarse grained water molecules. We employed periodic boundary conditions in all directions and independent thermostats (Berendsen[17] or v-rescale[18]) were applied to the solvent and the phospholipids to maintain their temperatures at the target values. The temperature coupling constant was set in all cases to 2 ps. The motion of the configuration center of mass was removed every 10 time steps.

In our previous work,[14] we employed a Berendsen semi-isotropic barostat to simulate bilayers at different surface tensions. This barostat does not produce the correct statistical ensemble and therefore it is not possible to compute the area compressibility modulus from a fluctuation analysis of the membrane area. In this work, we have employed instead the semi-isotropic Parrinello-Rahman barostat.[19] We complemented these simulations with additional ones using the Berendsen thermostat in order to highlight the differences associated to the simulations with these two barostats. The time

TABLE I. Simulation parameters of the systems investigated in this work. γ_0 is the surface tension, L_x and L_y the box lateral lengths, $a_\parallel$ is the mean projected area per phospholipid, a_{CU} is the mean true area per phospholipid, N_{Phos} the number of phospholipid molecules per layer, ΔT production simulation time, and N_{CW} the number of configurations employed in the fluctuation analysis. The simulations at constant surface tension were performed using the Parrinello-Rahman and Berendsen barostats. $\langle L_z \rangle \approx 14.0$ nm for all systems.

γ_0 (mN/m)	$\langle L_x \rangle$ (nm)	$\langle L_y \rangle$ (nm)	$a_\parallel$ (nm^2)	a_{CU} (nm^2)	N_{Phos}	ΔT (μs)	N_{CW}
			Parrinello Rahman barostat				
0	12.60 ± 0.01	13.23 ± 0.02	0.6671 ± 0.0002	0.670 77 ± 0.0002	256	0.450	6 000
0	12.75 ± 0.01	13.40 ± 0.02	0.6663 ± 0.0002	0.670 52 ± 0.0002	500	0.376	5 334
0	21.83 ± 0.01	22.87 ± 0.02	0.6662 ± 0.0002	0.670 83 ± 0.0002	750	0.450	6 001
0	35.55 ± 0.01	37.42 ± 0.02	0.6653 ± 0.0002	0.670 87 ± 0.0002	2000	0.450	5 934
0	43.54 ± 0.01	45.80 ± 0.02	0.6648 ± 0.0002	0.670 81 ± 0.0002	3000	0.300	3 987
0	50.28 ± 0.01	52.89 ± 0.02	0.6650 ± 0.0002	0.670 78 ± 0.0002	4000	0.249	3 311
4.2 ± 0.2	50.68 ± 0.01	53.28 ± 0.01	0.6748 ± 0.0005	0.681 0 ± 0.0005	4000	0.252	3 367
7.5 ± 0.2	50.95 ± 0.01	53.60 ± 0.01	0.6825 ± 0.0005	0.685 5 ± 0.0005	4000	0.290	3 855
10.57 ± 0.2	52.40 ± 0.01	52.71 ± 0.01	0.6905 ± 0.0005	0.693 8 ± 0.0005	4000	0.263	4 293
15.2 ± 0.2	52.86 ± 0.01	53.17 ± 0.01	0.7027 ± 0.0005	0.705 7 ± 0.0005	4000	0.274	4 569
21.2 ± 0.2	53.55 ± 0.01	53.87 ± 0.01	0.7212 ± 0.0005	0.723 8 ± 0.0005	4000	0.253	4 054
27.51 ± 0.2	55.17 ± 0.01	55.50 ± 0.01	0.7431 ± 0.0005	0.750 8 ± 0.0005	4000	0.291	3 881
			Berendsen barostat				
0	12.52 ± 0.01	13.32 ± 0.02	0.6657 ± 0.0002	0.670 78 ± 0.0002	250	0.450	6 000
0	21.82 ± 0.01	22.89 ± 0.02	0.6661 ± 0.0002	0.670 74 ± 0.0002	750	0.450	5 334
0	25.16 ± 0.01	26.46 ± 0.02	0.6660 ± 0.0002	0.670 71 ± 0.0002	1000	3.975	5 301
0	43.68 ± 0.01	45.67 ± 0.02	0.6650 ± 0.0002	0.670 77 ± 0.0002	3000	0.343	4 569
0	50.27 ± 0.01	52.88 ± 0.02	0.6646 ± 0.0002	0.670 74 ± 0.0002	4000	2.1	10 000
10.0 ± 0.2	51.67 ± 0.01	53.32 ± 0.01	0.6888 ± 0.0005	0.692 4 ± 0.0005	4000	0.265	3 538
15.0 ± 0.2	52.71 ± 0.01	53.29 ± 0.01	0.7023 ± 0.0005	0.705 3 ± 0.0005	4000	0.264	2 851
27.3 ± 0.2	53.20 ± 0.01	55.96 ± 0.01	0.7441 ± 0.0005	0.746 2 ± 0.0005	4000	0.291	3 881

coupling constant for the barostat was 10 ps in all cases. We use 4.5×10^{-5} and 9.8×10^{-5} bar^{-1} for the pressure coupling in the bilayer plane and normal directions, respectively.

The bilayers were subjected to different surface tensions, in the interval 0-27.3 mN/m. The surface tensions were computed using the microscopic pressure tensor route, see Ref. 14 for further details. We did not find evidence for pore nucleation in the membranes. The simulation time step was set to 0.03 ps in all our computations. The fluctuation analysis was performed over N_{CW} configurations. To investigate the size dependence of the area per phospholipid and the area compressibility modulus, we performed a systematic analysis by varying the membrane cross sectional area and the number of lipids. The water content, defined as the water to phospholipid ratio, was kept close to 27 in all these simulations. Full details on the simulations parameters are given in Table I. All the simulations were performed with the GROMACS 4.5 simulation package.[20]

In the rest of the paper, we use $\sigma = \sqrt{A_{Phos}} = 0.816$ nm and $kT = \beta^{-1}$ as the units of length and energy. σ defines the average distance between the phosphate groups in a POPC tensionless membrane, at 320 K.

III. FLUCTUATION MODES OF BILAYER MEMBRANES

The analysis of the bilayer thermal fluctuations provides a powerful approach to quantify the membrane elasticity including all the relevant fluctuation modes, from mesoscopic to molecular ones (lipid protrusions), using a single computer simulation. Different approaches have been proposed to analyze the fluctuation spectrum.[21] Despite the different approach, all the methods should be consistent with the *macroscopic elastic* limit described by the Helfrich Hamiltonian.[9] We expect that deviations from the Helfrich predictions will be observed when the fluctuations include high wave number modes, like lipid protrusions.

The analysis of the fluctuations in computer simulations requires the construction of a mathematical surface $z = \xi(x, y) \equiv \xi(\mathbf{R})$ that defines the *instantaneous shape* (IS) of the membrane. To construct the IS, we choose a set of *pivots* that are defined by the positions of the phospholipid molecules. We find that the phosphate pseudoatoms in the POPC MARTINI model provide a good representation for the IS pivots. The *pivots* were selected according to their position in the *upper* or *lower* leaflet.[22] The mathematical surfaces $z = \xi^{up,low}(\mathbf{R})$ representing the instantaneous shape of the upper and lower leaflets are then constructed using a function that interpolates through the pivots' coordinates. We use here the same interpolation scheme as in our previous work.[14] First, we construct a two dimensional Delaunay triangulation (DT) using the phosphate pseudoatom coordinates projected on the membrane plane (x, y). The DT is then used to identify the nearest neighbors from each individual phosphate pseudoatom. Using this information, we construct the corresponding three dimensional triangulated surfaces, where the triangle edges join each pivot to its nearest neighbors. The triangulated surfaces define $z = \xi^{low}(\mathbf{R})$ and $z = \xi^{up}(\mathbf{R})$. We take into account the periodicity of the simulation box on the bilayer plane, defined by the box vectors, L_x and L_y, to represent each IS in terms of a Fourier

series,

$$\xi(\mathbf{R}, q_m) = \sum_{|\mathbf{q}|\le q_m} \hat{\xi}_q e^{i\mathbf{q}\cdot\mathbf{R}}, \tag{2}$$

where the wavevectors are defined by $\mathbf{q} = 2\pi(n_x/L_x, n_y/L_y)$, for $n_{x,y} = 0, \pm1, \pm2, \ldots$. For constant surface tension simulations, the cross sectional area, $L_x \times L_y$, and hence the lattice reciprocal vectors, $\mathbf{q}$, fluctuate along the trajectory, but the changes in $\mathbf{q}$ are less than 1% for $N_{Phos} = 4000$ and 4% for $N_{Phos} = 256$. Hence, we decided to calculate all the relevant statistics for the Fourier terms using a common scaled square modulus $(2\pi)^2(n_x^2 + n_y^2) = q^2 A_\parallel = q^2 L_x L_y$. This approach facilitates the representation of the fluctuations in terms of a single wavevector, $q\sigma$, where σ is again the mean lipid-lipid distance in the tensionless POPC membrane. Formally, we extend series (2) up to $|q| = 2\pi/\lambda_c$, with $\lambda_c = \sqrt{a_\parallel} \approx \sigma$ although the relevant analysis will involve only $|q|$ values well below that limit.

The equilibrium thermal fluctuations of $\xi^{\mathrm{up}}(\mathbf{R})$ and $\xi^{\mathrm{low}}(\mathbf{R})$ are computed using a large set of equilibrated independent configurations sampled along the simulation trajectory.[23] In a symmetric bilayer fluctuating around a planar configuration, all the $q > 0$ Fourier components must have zero mean values $\langle\hat{\xi}_q^{\mathrm{low}}\rangle = \langle\hat{\xi}_q^{\mathrm{up}}\rangle = 0$, hence their mean quadratic fluctuations are described by two real numbers, $\langle|\hat{\xi}_q^{\mathrm{up}}|^2\rangle = \langle|\hat{\xi}_q^{\mathrm{low}}|^2\rangle$, that define the fluctuations of each bilayer leaflet, which are identical, and $\langle\hat{\xi}_q^{\mathrm{up}}\hat{\xi}_q^{\mathrm{low}*}\rangle = \langle\hat{\xi}_q^{\mathrm{low}}\hat{\xi}_q^{\mathrm{up}*}\rangle$, that describes the coupling between the two phospholipid layers, with $\hat{\xi}_q^*$ being the complex conjugated of $\hat{\xi}_q$. These equalities make it possible to average out the results obtained from both monolayers, hence improving the statistics of our computations, hence we used $\langle|\hat{\xi}_q^{\mathrm{m}}|^2\rangle = \left(\langle|\hat{\xi}_q^{\mathrm{low}}|^2\rangle + \langle|\hat{\xi}_q^{\mathrm{up}}|^2\rangle\right)/2$.

The bilayer fluctuations are often analyzed using the so called undulatory and peristaltic modes. The *undulatory* (U) mode[24,25] describes the fluctuations of the mean surface, with $\hat{\xi}_q^{\mathrm{U}} = (\hat{\xi}_q^{\mathrm{low}} + \hat{\xi}_q^{\mathrm{up}})/2$, and its mean square fluctuation,

$$\langle|\hat{\xi}_q^{\mathrm{U}}|^2\rangle = \frac{1}{2}\langle|\hat{\xi}_q^{\mathrm{m}}|^2\rangle + \frac{1}{2}\langle\hat{\xi}_q^{\mathrm{low}}\hat{\xi}_q^{\mathrm{up}*}\rangle. \tag{3}$$

The *peristaltic* (P)[7] mode, $\hat{\xi}_q^{\mathrm{P}} = (\hat{\xi}_q^{\mathrm{low}} - \hat{\xi}_q^{\mathrm{up}})/2$, describes the fluctuations of the membrane thickness as

$$\langle|\hat{\xi}_q^{\mathrm{P}}|^2\rangle = \frac{1}{2}\langle|\hat{\xi}_q^{\mathrm{m}}|^2\rangle - \frac{1}{2}\langle\hat{\xi}_q^{\mathrm{low}}\hat{\xi}_q^{\mathrm{up}*}\rangle. \tag{4}$$

The use of Equations (3) and (4) in the high q *uncoupled regime* is problematic, as the uncorrelated *monolayer protrusions*[10] $\langle\hat{\xi}_q^{\mathrm{low}}\hat{\xi}_q^{\mathrm{up}*}\rangle \approx 0$ and therefore $\langle|\hat{\xi}_q^{\mathrm{U}}|^2\rangle \approx \langle|\hat{\xi}_q^{\mathrm{P}}|^2\rangle$. We note that these protrusions should not be included in an analysis of the collective membrane undulations.[14]

The mean area of the undulatory surface area $A_{\mathrm{U}} = \langle A^{\mathrm{U}}\rangle$ is often used to represent the fluctuating bilayer membrane.[12,13] Following the capillary wave theory,[26–28]

$$A_{\mathrm{U}} \equiv \langle A^{\mathrm{U}}\rangle = \left\langle \int d^2\mathbf{R}\sqrt{1 + \left|\nabla_{\mathbf{R}}\xi^{\mathrm{U}}(\mathbf{R})\right|^2}\right\rangle$$

$$\approx A_\parallel + \frac{A_\parallel}{2}\sum_{0<|\mathbf{q}|}^{q_u} q^2\langle|\hat{\xi}_q^{\mathrm{U}}|^2\rangle. \tag{5}$$

A_{U} is not a well defined quantity because it depends on the upper limit $q \le q_{\mathrm{u}}$ appearing in the sum over the fluctuating modes. For high q_{u}, A_{U} increases with q_{u} due to the incorporation of *protrusion* terms. We illustrate this effect in Fig. 2, by representing the membrane roughness,

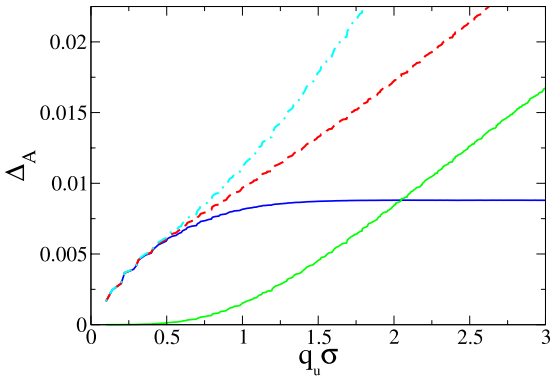

FIG. 2. The roughness of the membrane as function of the cutoff wavevector q_u, for the POPC free membrane ($\gamma_0 = 0$) with $N_{\mathrm{Phos}} = 4000$. The dark (blue) full line represents the coupled undulatory roughness $\Delta_{\mathrm{A}}^{\mathrm{CU}}$, the light (green) full line the peristaltic (uncoupled) roughness $\Delta_{\mathrm{A}}^{\mathrm{P}}$, the dashed line (red) the undulatory roughness $\Delta_{\mathrm{A}}^{\mathrm{U}}$, and the dashed-dotted line (cyan) the monolayer roughness $\Delta_{\mathrm{A}}^{\mathrm{m}}$.

$$\Delta_{\mathrm{A}}^{\alpha} \equiv \frac{\langle A^{\alpha}\rangle - A_\parallel}{A_\parallel}, \tag{6}$$

where α represents the corresponding fluctuation model.

This problem is also present in the estimation of A_{U} using the capillary wave theory. This can be shown by ~~first~~ assuming that each fluctuation mode fulfills the equipartition principle for the mean elastic energy, $q^2\gamma^{\mathrm{U}}(q)A_\parallel\langle|\hat{\xi}_q^{\mathrm{U}}|^2\rangle/2 = kT/2$, where $\gamma^{\mathrm{U}}(q)$ is a q-dependent surface tension, formally defined as $\langle|\hat{\xi}_q^{\mathrm{U}}|^2\rangle$, and ~~second~~ approximating the latter by the expansion,

$$\gamma^{\mathrm{U}}(q) \equiv \frac{k_{\mathrm{B}}T}{q^2\langle|\hat{\xi}_q^{\mathrm{U}}|^2\rangle A_\parallel} = \gamma_0 + \kappa q^2 + O(q^4), \tag{7}$$

where the bending modulus, κ, is responsible for the increase of the membrane stiffness $\gamma^{\parallel}$ with q with respect to the $q = 0$ ~~limit~~ value, which corresponds to the thermodynamic surface tension. Using Eq. (7), Eq. (5) can be rewritten as

$$A_{\mathrm{U}} - A_\parallel \approx \frac{1}{2}\sum_{0<|\mathbf{q}|}^{q_u}\frac{1}{\beta\gamma^{\mathrm{U}}(q)} \approx \frac{kT}{2}\sum_{0<|\mathbf{q}|}^{q_u}\frac{1}{\gamma_0 + \kappa q^2}, \tag{8}$$

showing that A_{U} increases with the wavevector q_{u} (see our simulated A_{U} in Fig. 2). Traditional approaches have attempted to resolve the area divergence problem discussed above by introducing an *ad hoc* cutoff for q in the sums of equations (5) and (8). The cutoff can be used to separate undulation and protrusion modes. Unfortunately, there is no general agreement on what cutoff value must be used. Different authors have used $2\pi/\sqrt{a_\parallel}$,[12] where $a_\parallel$ is the projected area per lipid, or $2\pi/d$,[7] where d is the membrane thickness. The first cutoff results in a very small system size dependence for the area per lipid, while for the second cutoff this dependence is stronger. Braun *et al.*[29] used a 1.15 nm^{-1} cutoff in simulations for DMPC, and in a subsequent work,[30] the same authors used a cutoff of 1.0 nm^{-1} for DOPC. Both values are lower than $2\pi/d$.

Although it is not often used in practical calculations, it is also possible to define a peristaltic area, A_P, by replacing $\xi^U(\mathbf{R})$ by $\xi^P(\mathbf{R}) = (\xi^{sup}(\mathbf{R}) - \xi^{inf}(\mathbf{R}))/\mathbf{2}$ in Eq. (5). We show in Fig. 1 that A_P represents the area of the leaflets when the membrane is forced to adopt a planar mean shape, i.e., $\hat{\xi}_q^U = 0$ and therefore $A_U = A_\parallel$ without changing the local distances between the two leaflets. The U surface (see Fig. 1) includes the proper undulatory component, and also, with half of their amplitude, the uncorrelated protrusions in each leaflet. The P surfaces do not include any contributions from the correlated undulation, for which $\langle|\hat{\xi}_q^m|^2\rangle \approx \langle\hat{\xi}_q^{low}\hat{\xi}_q^{up*}\rangle$, but feature the same behavior observed in the protrusions, where the amplitude of the latter is 1/2 of that observed in the leaflets, since they correspond to uncorrelated fluctuations with $\langle|\hat{\xi}_q^m|^2\rangle \gg \langle\hat{\xi}_q^{low}\hat{\xi}_q^{up*}\rangle$. We propose to eliminate the unwanted contribution to A_U arising from the uncorrelated protrusions. We exploit the fact that the same contribution appears in A_P, as shown by the parallel growth of A_U and A_P in Fig. 2 for $q_u\sigma > 1$. In this way, we may define a true undulating area given by Equation (1), which circumvents the problems associated to the selection of arbitrary values for q_u.

IV. A NEW ROUTE TO OBTAIN THE TRUE AREA OF BIOLOGICAL MEMBRANES

Our approach is based on the analysis of the CU mode introduced in our previous work.[14] The mean square fluctuations of this mode are given by

$$\langle|\hat{\xi}_q^{CU}|^2\rangle \equiv \langle|\hat{\xi}_q^U|^2\rangle - \langle|\hat{\xi}_q^P|^2\rangle = \langle\hat{\xi}_q^{low}\hat{\xi}_q^{up*}\rangle, \qquad (9)$$

which differs from the usual undulatory mode $\langle|\hat{\xi}_q^U|^2\rangle$. The CU mode uses the correlations between the phospholipids located in the two bilayer leaflets as a natural filter to quantify the global membrane undulations "only," hence overcoming the problems associated to the inclusion of protrusion contributions and avoiding the need to use a cutoff q_u. In our previous work,[14] we showed that the tension γ_0 obtained by fitting the CU spectrum at low q to the equation $\gamma^{CU}(q) = \gamma_0 + \kappa q^2$ agrees well with the surface tension imposed in the simulations and the one computed from the microscopic pressure tensor route. For the present bilayer, we obtained the bending modulus $\beta\kappa = 21$. Also, we showed that the CU mode is not sensitive to whether the Fourier or the real-space calculation is employed, and to the reference group used for define the monolayers surfaces.

Within the quadratic approximation, and similarly to Eq. (5) for A^U, the CU area is given by

$$A_{CU} \equiv \langle A^{CU}\rangle = A_\parallel + \frac{A_\parallel}{2}\sum_{0<|\mathbf{q}|}^{q_u} q^2\langle\hat{\xi}_q^{low}\hat{\xi}_q^{up*}\rangle. \qquad (10)$$

It can be shown that Eq. (9) along with Eq. (10) is equivalent to the geometrical definition given in Eq. (1). Equations (1) and (10), provide a new definition for the true area. We show in Fig. 2 that our new roughness, Δ_A^{CU}, is independent of q_u for $q_u\sigma \gtrsim 1$, as a result of the cancellation of A_U and A_P in Eq. (1). At low q_u, $A_P = A_\parallel$ and both CU and U agree with each other. The independence of the CU roughness with q_u cutoff for $q_u\sigma \gtrsim 1$ makes it possible to obtain the true area of the membrane.

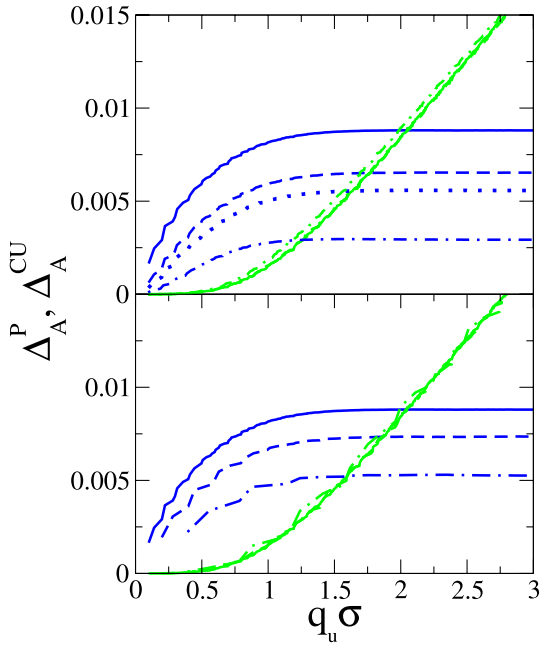

FIG. 3. The CU, dark (blue) lines, and P, light (green) lines, roughness of the membranes as function of the cutoff wavevector q_u. All results were obtained with the Parrinello-Rahman barostat. Top panel: membranes with $N_{Phos} = 4000$ at $\gamma_0 = 0.0$ mN/m (full lines), 4.2 mN/m (dashed lines), 7.5 mN/m (dotted lines), and 27.5 mN/m (dotted-dashed lines). Bottom panel: membrane in the tensionless state($\gamma_0 = 0$) as a function of the lateral size of the simulation box. Dashed-dotted lines: $L_x \approx 12.5$ nm ($N_{Phos} = 256$), dashed lines: $L_x \approx 25.0$ nm ($N_{Phos} = 1000$), and full lines: $L_x \approx 50.0$ nm ($N_{Phos} = 4000$). The overlap of the P data shows that this mode does not depend on the tension or the system size.

We have further analyzed the physical consistency of our approach by computing the membrane roughness of bilayers at different surface tension conditions (Fig. 3-top). The roughness obtained with our CU area, A_{CU}, features the correct dependence with the surface tension, namely, it decreases as γ_0 increases, and it does not depend on an arbitrary choice of the wavevector cutoff, $q_u\sigma > 1$, since Equations (1) and (10) eliminate the molecular scale fluctuations. In contrast, the area, A_P, obtained with the peristaltic mode, which describes an internal fluctuation of the bilayer, does not vary significantly with the membrane surface tension, but it increases with increasing q_u, reflecting the inclusion of contributions associated to lipid individual protrusions (see Fig. 3). We have shown so far that (1) the CU mode fulfills the physical laws governing membrane fluctuations, namely, increasing roughness with decreasing surface tension, (2) that the peristaltic P contribution is an invariant internal property of the membrane, and (3) the thermodynamic conjugate variable of the surface tension is the area, and not the peristaltic changes in the membrane thickness. As shown in Fig. 3, A_P is nearly invariant with the surface tension; therefore, an improper contribution of the peristaltic mode to the area may lead to failures in the thermodynamic consistency.

We analyze now the area per phospholipid, which is one of the most important properties defining the structure of biological membranes, and widely used to test the accuracy of simulation forcefields. We have computed the area per lipid

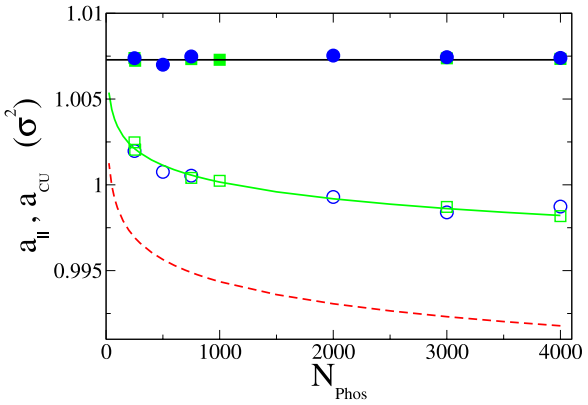

FIG. 4. The area per phospholipid for the free membrane *vs.* the number of phospholipid, $N_{\rm Phos}$ (lateral size of the box simulation). The full symbols represent the CU areas, $a_{\rm CU} = A_{\rm CU}/N_{\rm Phos}$, and the empty symbols the projected areas $a_{\parallel} = A_{\parallel}/N_{\rm Phos}$. The circles (blue) show the results obtained with the Parrinello-Rahman barostat and the squares (green) with the Berendsen barostat. The full line shows the fit to the logarithmic behavior predicted by Eq. (11). The dashed (red) line represents the behavior of $a_{\parallel}$ predicted by Eq. (11) with $a_{\rm true} = a_{\rm CU} = 1.0074\sigma^2$ and $\beta\kappa = 21$.

using the CU analysis introduced in this work and the projected area per lipid, $a_{\parallel} = A_{\parallel}/N_{Phos}$, which also represents the projected area of our true area $a_{\rm CU}$. We show in Fig. 4 the system size dependence of the area per lipid computed using both the Berendsen and Parrinello-Rahman barostats. The CU area per lipid, $a_{\rm CU}$, is independent of system size while the projected area per lipid, $a_{\parallel}$, widely used in computer simulation studies decreases as the membrane size increases. Equation (10) shows that the bilayer maintains a constant CU area per lipid by reducing the projected area per lipid when the bilayer size increases, to compensate the increase of the q dependent term in Eq. (10). We conclude that $A_{\rm CU}$ is a proper thermodynamic variable in our simulations of the free membrane. It is important to note that according to Equation (6), the insensitivity of $a_{\rm CU}$ to membranes size shows that the roughness does depend on the system size, as illustrated in Fig. 3-bottom. Larger membranes result in a larger CU roughness, $\Delta_{\rm A}^{\rm CU}$, since they have smaller projected areas per lipid. Moreover, we note that $\Delta_{\rm A}^{\rm P}$ does not vary with the system size, because $A^{\rm P}$ is proportional to the projected area.

The method presented above provides a "direct" route to compute the true area per lipid in biological membranes. Alternative methods require "indirect" approaches to extract the true area. These methods rely on the theoretical estimation of the undulatory contribution to $A_{\parallel}$, as predicted by Eq. (8). In the latter, the sum over wavevectors is approximated by an integral from a lower limit $q_{\rm size} = 2\pi/L_x$, defined by the system size, to an upper limit, $q_{\rm u}$, defined by a characteristic molecular length scale. Waheed and Edholm[12] used the relationship $(q_{\rm u}/q_{\rm size})^2 \approx N_{\rm Phos}$ to obtain the equation

$$A^{true} = A_{\parallel}\left(1 + \frac{k_B T}{8\pi\kappa}\ln\left(N_{Phos}\right)\right). \qquad (11)$$

The logarithmic dependence of this equation with the number of phospholipids in the membrane agrees qualitatively with our results (see solid line in Fig. 4), but only when the bending modulus, κ, and the true area are taken as fitting parameters. As shown by the dashed line represented in Fig. 4 (using the bending modulus $\kappa = 21kT$), Eq. (11) predicts a difference between a^{true} and $a_{\parallel}$ about 0.2% larger than that is found for our $a^{\rm CU}$, which on the scale of the figure represents a large shift. This discrepancy is connected to the sum over q appearing in Eq. (8). This sum has to be replaced by an integral and truncated at q_u, in order to recover the $ln(N_{Phos})$ functionality. For membranes with $N_{Phos} \lesssim 1000$, Eq. (11) only gives a qualitative dependence. Amongst the most recent alternatives,[13,29,30] Otter[13] employed a more sophisticated approach, which relies on a triangulation procedure to compute the area of large membranes, hence avoiding the drawbacks associated to the evaluation of the sum over q. He obtained the area per molecule from the asymptotic limit of the area for very large system sizes.

Our area per lipid $a = 0.6707 \pm 0.0005$ nm^2 for the free membrane is very similar to the one reported in the POPC experiments of Hyslop *et al.*[31] at 310 K, 0.66 nm^2, slightly larger than the area reported by Smaby *et al.*[32] at 297 K, 0.63 nm^2, and slightly lower than the area obtained by Kucerka *et al.*[33] at 303 K, 0.683 nm^2. The differences across experiments may be connected to the difference experimental approaches. It is known that the areas obtained using neutron, X-rays, or ~~NMR~~ techniques may be different, hence adding uncertainty to the use of this quantity as a reference for force-field fitting and testing.[34] The simulations of Braun *et al.*[30] using a similar lipid (DOPC) at T = 303 K predict area of $a = 0.659$ nm^2, after filtering out the non-undulatory modes with $q > 1$ nm^{-1}, which is used by these authors to define their "undulation reference surface." We find that our true area per lipid is in good agreement with previous simulations of the projected area per lipid, $a_{\parallel}$, as well as our own computations of this quantity, $a_{\parallel} = 0.666 \pm 0.002$ nm^2 (See Table I). The latter result is very close to previous simulations using the AMBER forcefield at 303 K, $a_{\parallel} = 0.668$,[35] and similar to the results reported by Janosi using the ~~CHARMM~~ forcefield at 310 K, $a_{\parallel} = 0.647 \pm 0.013$ nm^2,[36] and by Poger using the GROMOS96 forcefield at 303 K, $a_{\parallel} = 0.638$.[37]

The comparison above shows that there are very small differences between the true area per lipid and the projected one (see the scale of the y axis in our Fig. 4). Hence, it is clear that the projected area, $a_{\parallel}$, provides a good approximation to the true area per molecule in many situations. However, computations requiring accurate areas (see, e.g., the data in Table I of Ref. 12) cannot rely on the projected area. Our method provides a route to compute the true area using very small bilayers (see, e.g., $N_{Phos} = 256$ system in Fig. 4) and a single simulation, hence avoiding the need to compute the bending modulus, and the problems associated to the evaluation of the sums over the q corrugation modes.

V. CHARACTERISTIC RELAXATION TIME OF THE AREA FLUCTUATIONS

To get a better insight into the differences between $A_{\rm CU}$ and $A_{\parallel}$ modes, we computed the time correlation functions of these two areas. The correlation function is defined as

$$\Gamma(t) = \frac{\langle (A(t) - \langle A\rangle)\,(A(t=0) - \langle A\rangle)\rangle}{\langle (A(t=0) - \langle A\rangle)^2\rangle}. \qquad (12)$$

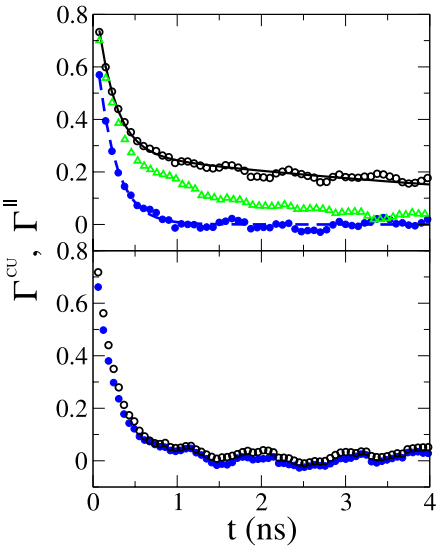

FIG. 5. The normalized area autocorrelation function $\Gamma(t)$ Eq. (12) for the projected area, empty (black) circles, and for the CU area, full (blue) circles, for membranes with $N_{\text{Phos}} = 4000$. Top panel: tensionless membranes. Γ^{CU} shows a faster exponential decay, $\Gamma^{\text{CU}}(t) \approx 0.786 exp(-t/0.222)$ (dashed line), than $\Gamma^{\|}(t) \approx 0.654 exp(-t/0.222) + 0.274 exp(-t/6.775)$ (full line). The (green) triangles represent $\Gamma^{\|}$ for a smaller membrane, $N_{\text{Phos}} = 2000$. Bottom panel: membrane under tension, $\gamma_0 = 10.57$ mN/m.

We show in the top panel of Fig. 5 the results for the $N_{\text{Phos}} = 4000$ system in the tensionless state. The isobaric simulations were performed using the Parrinello-Rahman barostat. The CU area behavior is consistent with the one expected for a proper thermodynamic property, namely, the fluctuations decay exponentially with a short relaxation time $\tau_{\text{CU}} \approx 0.22$ ns making possible the determination of the mean area $\langle a_{\text{CU}} \rangle$ using short simulation times, irrespective of the system size. In contrast, the relaxation of the projected area, $A_{\|}$, follows a double exponential relaxation, with one of the exponentials featuring the same relaxation time as obtained from the CU mode, τ_{CU}. The second contribution to $\Gamma^{\|}(t)$ corresponds to a much slower decay time $\tau_{\|} \approx 30\tau_{\text{CU}}$, which is connected to changes of the membrane shape that are not related to the fluctuations of the true area, A^{CU}. That indicates that changes in the second term of Eq. (10) are counteracted by changes in $A_{\|}$ (the first term of Eq. (10)) and therefore do not modify A^{CU}. This second decay of the $A_{\|}$ fluctuations slows down as the membrane size increases. Hence, larger simulations would be necessary to get an accurate estimation of the mean value $\langle a_{\|} \rangle$ for larger membranes. We test this idea in the top panel of Fig. 5. The triangles represent $\Gamma_{\|}$ for a smaller membrane, $N_{\text{Phos}} = 2000$ instead 4000. Our results shows that $\tau_{\|}$ indeed decreases with membrane size. In fact for $N_{\text{Phos}} = 5000$ $\tau_{\|}$ and τ_{CU} become of the same order.

We have further analyzed the impact of the membrane tension on the relaxation time. We find that applying a tension reduces the dependence of the relaxation time with system size. We show in the bottom panel of Fig. 5 that the double-exponential dependence of the projected area is eliminated and the time correlation functions for the CU and projected areas agree with each other, hence featuring similar relaxation times. We note that the tension modifies the projected area time dependence while the CU remains unchanged.

Finally, we have analyzed the impact of the barostat either Berendsen or Parrinello-Rahman, on the relaxation of the area fluctuations. We find that the slow relaxation mode of $A_{\|}$ is fairly independent on the barostat used, while the relaxation of the A_{CU} mode is very sensitive to the barostat, with the relaxation time for the Berendsen case being twice as long as the one obtained with the Parrinello-Rahman approach. This result clearly shows that the barostat influences the membrane fluctuation dynamics, and care should be exercised when computing dynamic properties involving area fluctuations.

VI. THE AREA COMPRESSIBILITY MODULUS

The area compressibility modulus measures the isothermal variation of the surface tension with the membrane area. It also quantifies the mean square thermal fluctuations per unit area as

$$K = A\left(\frac{\partial \gamma}{\partial A}\right)_T = \frac{kT\,A}{\langle A^2 \rangle - \langle A \rangle^2}. \tag{13}$$

These equations may be applied to any definition of the membrane area, either A^{U}, $A^{\|}$, or A^{CU}. The evaluation of the compressibility with the U mode is problematic, as the average area, $\langle A^{\text{U}} \rangle$, depends on the wavevector cutoff used to separate undulations and molecular protrusions. The projected area provides a simple alternative to estimate compressibility from computer simulations. However, as shown above the projected area, $A^{\|}$, fluctuations depend on the system size. Hence, the evaluation of the corresponding compressibility, $K^{\|}$, via a direct derivative or the area fluctuations (see Eq. (13)) will be affected by the unphysical behavior of $A^{\|}$. In contrast, we argue that the CU area is a well defined thermodynamic quantity that provides a consistent, physically meaningful approach to calculate K^{CU}. We revise in the following these approaches and their consistency by investigating their performance in compressibility computations, either via the derivative of the surface tension (the Hooke approach) or via the analysis of the area fluctuations.

A. The Hooke approach

The area compressibility of an equilibrium tensionless ($\gamma_0 = 0$) membrane, with mean area $A(\gamma_0)$, may be obtained from Eq. (13) by calculating the increase of the area induced by an applied small tension, $\gamma_0 > 0$. The area increase, α, is given by

$$\alpha \equiv \frac{A(\gamma_0) - A(\gamma_0 = 0)}{A(\gamma_0 = 0)} \approx \frac{\gamma_0}{K}. \tag{14}$$

This equation may be used, either with the projected or the true CU area, to estimate the $K^{\|}$ and K^{CU} compressibility moduli. In order to use this method, we need first to find the range of validity of the linear Hooke's law. We show in Fig. 6 that our CU data do indeed follow the expected linear dependence up to $\alpha^{\text{CU}} \lesssim 0.05$ and $\gamma_0 \lesssim 0.015$ N/m. At higher surface tensions, γ_0, a deviation from linearity can be observed, signaling the onset of the non-elastic response of the membrane. We recall that all the results discussed in the present section were obtained with the Parrinello-Rahman barostat, although our

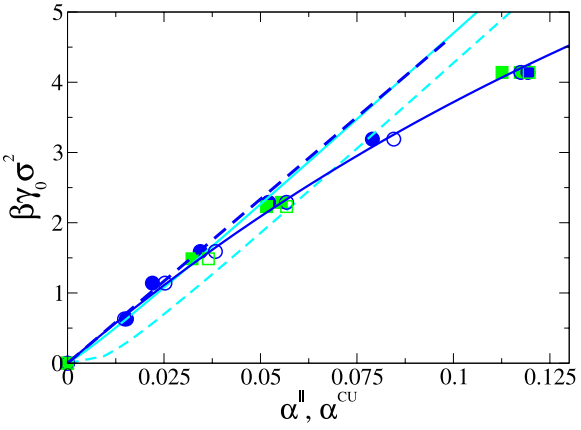

FIG. 6. The normalized area expansion α (defined by Eq. (14) in the main text) *vs.* tension for membranes consisting of $N_{\text{Phos}} = 4000$. The full symbols show the results for the CU area, α^{CU}, and the empty symbols for the projected area, $\alpha^{\|}$. The (blue) circles show the results obtained with the Parrinello-Rahman barostat and the (green) squares with the Berendsen barostat. The dashed (blue) dark line represents a linear fit ($y = 46.72x$) to the low $\beta\gamma_0\sigma^2 < 2.0$ values obtained with the Parrinello-Rahman barostat for α^{CU}. The full (blue) dark line represents α^{CU} evaluated by integrating the linear dependence of K with γ_0 as obtained in Fig. 8, see Eq. (19). The light (cyan) full line is the fit of the low γ_0 values of $\alpha^{\|}$ to Eq. (15), using for the bending modulus $\beta\kappa = 21$. The light (cyan) dashed line represent the predictions of Eq. (15) for a system with an area one hundred times greater than the one used in our computations.

results for α^{CU} are independent of the barostat employed, as we can see in Fig. 6. By fitting the linear regime in Fig. 6, we can extract the compressibility modulus, $\beta K^{\text{CU}}\sigma^2 = 46.72$, which corresponds to a compressibility of $K^{\text{CU}} = 0.31 \pm 0.02$ N/m, well within the range of values reported for lipid and cell membranes.[38] Our estimated error for K^{CU} represents the difference between the linear fits over the range of the lowest two, three, or four values of γ_0.

Traditionally, the compressibility has been computed by analyzing the projected area, $A_{\|}$. As noted in Sec. ~~V~~, in the tensionless state, $\gamma_0 = 0$, $A_{\|}$ is not extensive (see Fig. 4). The equilibrium fluctuations of the free membrane induce a reduction of the projected area per phospholipid, $a_{\|}$, since the plane tangential to a point on the membrane surface may take any orientation with respect to the plane, (x, y), where the bilayer surface is projected. A very small tension ($\gamma_0 > 0$) can induce a large increase in the mean projected area with respect to the tensionless case. This issue has been noted before by Rawicz *et al.*[39,40] These authors used the ~~CWT~~ to derive a relationship that describes the dependence of the projected area with the membrane surface tension, γ_0, by considering the undulations featured by large membranes,

$$\alpha^{\|} \equiv \frac{A_{\|}(\gamma_0) - A_{\|}(\gamma_0 = 0)}{A_{\|}(\gamma_0 = 0)} = \frac{1}{8\pi\beta\kappa} \ln\left(1 + \frac{\beta\gamma_0 A_{\|}}{4\pi^2\beta\kappa}\right) + \frac{\gamma_0}{K^{\text{true}}}. \quad (15)$$

The derivative of $\alpha^{\|}$ with respect to the surface tension, γ_0, under tensionless conditions $\gamma_0 = 0$ gives

$$\frac{1}{K^{\|}} = \frac{1}{K^{\text{true}}} + \frac{A_{\|}(\gamma_0 = 0)}{c\pi^3\beta\kappa^2}, \quad (16)$$

which is similar to the equation derived by Waheed and Edholm,[12] from the fluctuation analysis of the projected area, $\langle A^{\|2}\rangle - \langle A^{\|}\rangle^2$. These authors pointed out that the numerical coefficient c, which would be exactly 32 for Eq. (16), depends on the procedure used to evaluate the sum of the Eq. (8) over the low wavevectors.[12] According to Eq. (16), the effective area compressibility, $K^{\|}$, vanishes when the membrane reaches the thermodynamic limit, $A_{\|} \to \infty$. The influence of the undulations on the compressibility, and the corresponding differences between the Hookean $K^{\|}$ and K^{true}, would be observed when the derivative of $\alpha^{\|}$ is evaluated for surface tensions fulfilling $\beta\gamma_0\sigma_0^2 \ll 4\pi^2\beta\kappa/N_{\text{Phos}}$. In our largest simulations, consisting of $N_{\text{Phos}} = 4000$, we have $4\pi^2\beta\kappa/N_{\text{Phos}} \approx 0.2$, where we used the bending modulus $\beta\kappa \approx 21$ obtained in our previous work.[14] Therefore for the range explored here $0.5 \lesssim \beta\gamma_0\sigma^2 \lesssim 2.5$, our data follow Eq. (14) within the accuracy of our computations, namely,

$$\alpha^{\|} - \alpha^{\text{CU}} \approx \frac{1}{8\pi\beta\kappa} \ln\left(1 + \frac{\beta\gamma_0 A_{\|}}{4\pi^2\beta\kappa}\right) \lesssim 3 \times 10^{-3}. \quad (17)$$

We have represented in Fig. 6 the predictions of Eq. (15) for a hypothetical system consisting of $N_{\text{Phos}} = 4 \times 10^6$ phospholipid molecules. It is evident that $\beta\gamma_0\sigma^2$ does not change linearly with $\alpha^{\|}$ at low $\alpha^{\|}$. This deviation from linearity has a very little impact on the compressibility, $K^{\|}$, obtained from Hooke's law (Eq. (14)), for $\beta\gamma_0\sigma^2 \approx 1$ (see Fig. 6).

In simulations consisting of less than 4000 lipids per layer, and for the values of γ_0 studied here, $A_{\|}$ is not large enough for the first term in Eq. (15) to play a significant role. The differences between $\alpha^{\|}$ and α^{CU} are small and the behavior of $A_{\|}$ can be well approximated directly by the Hookean law, Eq. (14). Nonetheless, we have calculated K^{true} by fitting our $\alpha^{\|}$ data for low γ_0 to the theoretical expression given by Eq. (15), using again our previous result $\beta\kappa = 21$. We show in Fig. 6 the corresponding fit. From this fit, we find $\beta K^{\text{true}}\sigma^2 = 50.0$ and $K^{\text{true}} = 0.331$ N/m, which is close to the value obtained from the analysis of the true CU area, 0.31 ± 0.02 N/m.

B. The area fluctuation approach

The evaluation of the area compressibility modulus from area fluctuations (13) is much more sensitive to the area definitions than the Hookean approach. As discussed above, the fluctuations of the projected area are strongly affected by the boundary conditions in the tensionless state. We have computed the compressibility using both the projected and the CU definition of the true area, as well as the two different barostats, i.e., Rahman-Parrinello and Berendsen. We find that the barostat type has a significant impact on the results.

For the tensionless membrane, see Fig. 7, the CU compressibility obtained with the Parrinello-Rahman barostat features a remarkable independence with the membrane area, for a wide range of values, from 200 nm^2 to 3000 nm^2. The resulting average compressibility, $K^{CU} = 0.31$ N/m, is in excellent agreement with the value obtained from the Hookean analysis, $K^{\text{CU}} = K^{\|} = 0.31 \pm 0.02$ N/m. Our result clearly shows that the combination of a barostat that produces the correct ensemble fluctuations combined with the true area definition proposed here predicts area compressibility moduli

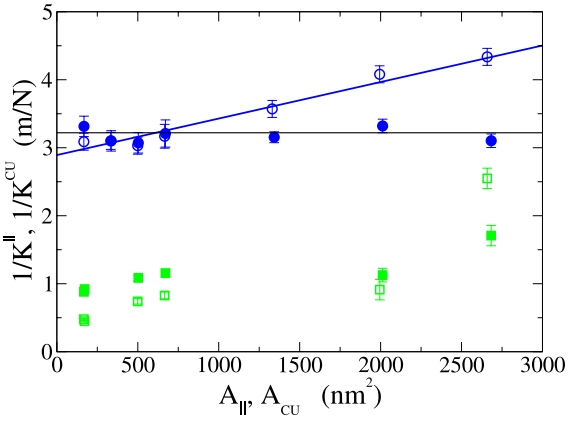

FIG. 7. The dependence of the inverse of the area compressibility modulus K with system size for a tensionless membrane. The compressibility was obtained from an area fluctuation analysis. The open symbols represent the compressibility obtained from the projected area, $K^{\parallel}$, and full symbols the results obtained from the analysis of the CU area, K^{CU}. The (blue) circles represent data obtained with the Parrinello-Rahman barostat and the (green) squares with the Berendsen barostat. The (blue) line represents the linear fit of the $K^{\parallel}$ values obtained with the Parrinello-Rahman barostat, i.e., to the (blue) empty circles. The horizontal line (black) indicates the compressibility obtained using Hooke's law. (see Section VI A).

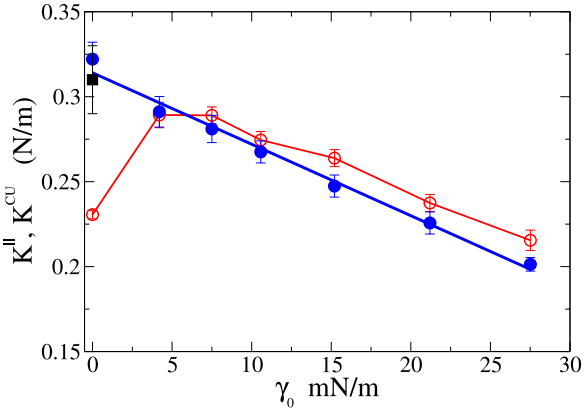

FIG. 8. Dependence of the area compressibility modulus with the membrane surface tension γ_0, for a membrane consisting of $N_{\mathrm{Phos}} = 4000$ lipids. The simulation results were obtained using the Parrinello-Rahman barostat. Full (blue) symbols represent the results obtained with the CU area, K^{CU}, and empty (red) symbols the results obtained from the projected area, $K^{\parallel}$. The thick (blue) line represents a linear fitting to the K^{CU} values, and the thin (red) line is a guide to the eye. The square (black) indicates the compressibility at $\gamma_0 = 0$ obtained from Hooke's law (see Section VI A).

in perfect agreement with the Hookean route. The Berendsen barostat on the other hand does not produce the correct fluctuations, and this is reflected in the strong overestimation of the area compressibility modulus with respect to the Hookean prediction. Hence, in the following, we will discuss the results obtained with the correct barostat, Parrinello-Rahman, only.

The compressibility $K = 0.31 \pm 0.02$ N/m falls within the range of values reported in experiments, 0.18-0.30 N/m.[41] Our result is close to that reported by Janosi and Gorfe for POPC bilayers,[36] 0.272 N/m, although this value was obtained using a different force-field (CHARMM) and from the fluctuations of the projected area, which as we shall see below is inaccurate. Braun *et al.*[30] employed the Hookean approach and reported a value of $K = 0.277 \pm 0.01$ N/m for a similar lipid (DOPC) at T = 303 K.

We show in Fig. 7 our results for the fluctuations of the projected area using the Parrinello-Rahman barostat. The area compressibility shows a clear dependence with system size, which can be fitted to the linear dependence of $1/K^{\parallel}$ with $A^{\parallel}$ predicted by Eq. (16). The linear fitting, using again as bending rigidity $\beta\kappa = 21$, shows good agreement with the theoretical predictions of Eq. (16). The numerical factor $c \approx 33$ is very close to 32 predicted by Eq. (15). The extrapolation of the compressibility to zero area (see Fig. 7) gives $K^{true} = 0.34$ N/m, slightly higher than the value obtained directly from our analysis of the A_{CU} area fluctuations. We conclude that although the traditional methods based on Eq. (16) give acceptable values of K, the use of the true area A_{CU} is more robust as the compressibility is independent of system size, making it possible to compute this property from a single simulation.

Finally, the area compressibility modulus defined in (13) may also be obtained for membranes under tension. We examine in the following the dependence of K^{CU} and $K^{\parallel}$ with the bilayer tension γ_0. For this analysis, we considered large bilayers, consisting of 4000 lipids per leaflet. We show in Fig. 8 that the compressibility obtained from the true area (CU mode) or the projected area is very similar for $\gamma_0 > 2.5$ mN/m, although $K^{\parallel}$ is slightly larger than K^{CU}. It is only in the limit of very low tensions that the behavior of the compressibility modulus obtained from both areas differ. The results from the projected area deviate significantly as we approach the tensionless state, $\gamma_0 = 0$. Note that for these larger membranes, 4000 lipids, the inaccuracy of the projected area approach is particularly noticeable, as the tensionless state features a compressibility which is not in line with the ones obtained for membranes under tension. This failure of the projected area approach is reflected in a large drop of the compressibility in going from 5 mN/m (~0.3 N/m) to 0 mN/m (~0.23 N/m). On the other hand, K^{CU} increases linearly with decreasing surface tension and converges to the Hookean result of the tensionless state. A linear fit to our K^{CU} gives $K^{\mathrm{CU}}(\gamma_0) \approx K^{\mathrm{CU}}(\gamma_0 = 0) - 4.2(\pm 0.3)\gamma_0$. From this result, we may predict the area deformation as a function of the surface tension. Integrating Eq. (13),

$$\alpha^{\mathrm{CU}}(\gamma_0) = \frac{A(\gamma_0) - A(\gamma_0 = 0)}{A(\gamma_0 = 0)} = exp\left[\int_0^{\gamma_0} \frac{d\gamma}{K^{\mathrm{CU}}(\gamma)}\right] - 1, \tag{18}$$

and replacing the linear fit,

$$\alpha^{\mathrm{CU}}(\gamma_0) = \frac{\beta K^{\mathrm{CU}}(\gamma_0 = 0)\sigma^2}{(\beta K^{\mathrm{CU}}(\gamma_0 = 0)\sigma^2 - 4.2\beta\gamma_0\sigma^2)^{4.2}}, \tag{19}$$

which we have represented in Fig. 6. The prediction is fully consistent with the direct calculation of the mean area for the whole range of areas, including those beyond the linear Hookean range. The consistency of the fluctuation and Hookean routes highlights again that our definition of A_{CU} measures the true area of the undulating membrane.

In a recent work,[42] the authors considered the error associated to the estimation of K_A from the analysis of $\Delta\alpha$ vs γ when the tilt is ignored. It would be very interesting to

check whether the tilt modes may explain the dependence of the compressibility with the surface tension observed in our computations.

VII. CONCLUDING REMARKS

In this work, we have reported a new approach to compute the true area of a membrane under tension and in the tensionless state. Our approach circumvents the problems associated to existing approaches, which either rely on the computation of the membrane area using the undulatory modes, A_U, which is given by the average position of the lipid head groups, or, more simply, via the projected area, $A_\parallel$. The former approach is affected by protrusion contributions, while the latter is thermodynamically inconsistent, since the projected area is not extensive. The true area proposed here is defined in terms of a coupled undulatory area,

$$A_{CU} = A_U - (A_P - A_\parallel), \tag{20}$$

which allows to completely eliminate the protrusion contributions and to recover thermodynamic consistency. We have tested our approach by performing molecular dynamics simulations of POPC membranes using the MARTINI force field. We have demonstrated that the CU area per lipid and the area compressibility K^{CU} do not depend on the lateral size of the simulation box for a wide range of system sizes. This result opens the route to accurately compute the true area per lipid and compressibility using truly small bilayer patches, down to 500 lipids. Further, we have shown that the CU relaxation time associated to the bilayer area fluctuations does not depend of the system size, while the projected one increases with the membrane size. For $N_{Phos} = 4000$, the projected area relaxation time is one order of magnitude larger that the CU one.

We have tested the thermodynamic consistency of the compressibility, K^{CU}, obtained from the true area, A^{CU}. With this purpose, we applied the Hookean and area fluctuation approaches to membranes under tension and in the tensionless state. We found agreement between these two approaches. Our results indicate that the thermodynamic consistency extends beyond the elastic regime. Our areas per lipid and compressibilities for MARTINI POPC bilayers are in line with previous computations for the tensionless state, $a = 0.6707 \pm 0.0005$ nm^2 and $K = 0.31 \pm 0.02$ N/m. The compressibility results are, as expected, strongly dependent on the barostat employed. The Nosé-Hoover barostat reproduces the correct fluctuations of the ensemble, and the compressibilities obtained from these fluctuation and from the direct approach, namely, Hooke's law, are fully consistent. As expected, the compressibility obtained from the analysis of the area fluctuations using the Berendsen barostat, which is widely employed in computer simulations, is not consistent with the Hooke's approach.

One main advantage of our approach is that it obviates the need to perform a series of simulations at different membrane areas, and/or pre-computations of the bending modulus, which are required in current approaches to assess system size effects and to quantify the compressibility in the thermodynamic limit. Further, we have tested the accuracy of ~~equation~~ ~~of~~ Rawicz *et al.*, which estimates the true area compressibility from an analysis of the system size dependence of the projected area compressibility. Our results confirm previous observations[12,13] ~~of~~ showed that this equation is qualitatively correct.

Many computations in the past have been performed using the projected area. Interestingly, we find that the deviations of this area from the true one are small, ~1%-2%, for a wide range of system sizes, 10^2-10^3 lipids, probably within the uncertainty associated to the forcefields/experiments. However, the compressibilities of the tensionless membrane depend strongly on the system size, and for membranes consisting of $\sim 10^3$ lipids, the use of the projected area can lead to compressibilities that deviate significantly, ~30%, from the real value. Ironically, we have found that the projected area provides an interesting approach to "estimate" the area per lipid and compressibility when the bilayer size is small, ~500 lipids. However, as the use of the projected area for these small sizes is an uncontrolled approximation, it should be used with great care.

Overall, we have demonstrated that the computational approach presented in this work circumvents most of the problems of the existing methods, as it does not require *ad hoc* parameters, such as the cutoff employed in Fourier series methods, numerical prefactors employed in analytical equations, computations using several system sizes, or pre-computations of the bending modulus. More importantly, unlike the widely used project area, the CU area proposed here is thermodynamically consistent.

ACKNOWLEDGMENTS

We acknowledge the support of the Spanish Ministry of Science and Innovation (Grant Nos. FIS2010-22047-C05 and FIS2013-47350-C5). We would also like to acknowledge the Imperial College High Performance Computing Service for providing computational resources. FB would like to thank the EPSRC (No. EP/J003859/1) for the award of a Leadership Fellowship.

[1]J. Lundbaek, J. Phys.: Condens. Matter **18**, S1305 (1989).
[2]R. Kik, F. Leermakers, and M. Kleijn, Phys. Chem. Chem. Phys. **7**, 1996 (2005).
[3]H. Khandelia, J. Ipsen, and O. Mouritsen, Biochim. Biophys. Acta, Biomembr. **1778**, 1528 (2008).
[4]S. Marrink, A. de Vries, and D. Tieleman, Biochim. Biophys. Acta **1788**, 149 (2009).
[5]R. Goetz and R. Lipowsky, J. Chem. Phys. **108**, 7397 (1998).
[6]J. Neder, B. West, P. Nielaba, and F. Schmid, J. Chem. Phys. **132**, 115101 (2010).
[7]E. Lindahl and O. Edholm, Biophys. J. **79**, 426 (2000).
[8]S. Marrink and A. Mark, J. Phys. Chem. B **105**, 6122 (2001).
[9]W. Helfrich, Z. Naturforsch. C **28**, 693 (1973).
[10]R. Lipowsky and S. Grotehans, Europhys. Lett. **23**, 599 (1993).
[11]W. K. den Otter and W. J. Briels, J. Chem. Phys. **118**, 4712 (2003).
[12]Q. Waheed and O. Edholm, Biophys. J. **97**, 2754 (2009).
[13]W. K. den Otter, J. Chem. Phys. **123**, 214906 (2005).
[14]P. Tarazona, E. Chacón, and F. Bresme, J. Chem. Phys. **139**, 094902 (2013).
[15]S. Marrink, H. Risselada, S. Yefimov, D. Tieleman, and A. de Vries, J. Phys. Chem. B **111**, 7812 (2007).
[16]Y. Zhang, A. Lervik, J. Seddon, and F. Bresme, Chem. Phys. Lipids **185**, 88 (2015).
[17]H. Berendsen, J. Postma, W. van Gunsteren, A. DiNola, and J. Haak, J. Chem. Phys. **81**, 3684 (1984).
[18]G. Bussi, D. Donadio, and M. Parrinello, J. Chem. Phys. **126**, 014101 (2007).

[19]M. Parrinello and A. Rahman, J. Appl. Phys. **52**, 7182 (1981).
[20]B. Hess, J. Chem. Theory Comput. **4**, 435 (2008).
[21]C. Loison, M. Mareschal, K. Kremer, and F. Schmid, J. Chem. Phys. **119**, 13138 (2003).
[22]H. Martinez, E. Chacón, P. Tarazona, and F. Bresme, Proc. R. Soc. A **467**, 1939 (2011).
[23]E. Chacón and P. Tarazona, Phys. Rev. Lett. **91**, 166103 (2003).
[24]J. Israelachvili and H. Wennerstrom, J. Phys. Chem. **96**, 520 (1992).
[25]S. A. Safran, *Statistical Thermodynamics of Surfaces, Interfaces, and Membranes* (Addison-Wesley, Reading, MA, 1994).
[26]F. Buff, R. A. Lovett, and F. Stinger, Phys. Rev. Lett. **15**, 621 (1965).
[27]J. Percus, in *Fluid Interfacial Phenomena*, edited by C. Croxton (John Wiley, New York, 1986), pp. 1–44.
[28]R. Evans, Adv. Phys. **28**, 143 (1979).
[29]A. R. Braun, E. G. Brandt, O. Edholm, J. F. Nagle, and J. N. Sachs, Biophys. J. **100**, 2112 (2011).
[30]A. R. Braun, J. N. Sachs, and J. F. Nagle, J. Phys. Chem. B **117**, 5065 (2013).
[31]P. A. Hyslop, B. Morel, and R. Sauerheber, Biochemistry **29**, 1025 (1990).
[32]J. M. Smaby, M. Momsen, H. L. Brockman, and R. E. Brown, Biophys. J. **73**, 1492 (1997).
[33]N. Kucerka, S. Tristram-Nagle, and J. F. Nagle, J. Membr. Biol. **208**, 193 (2005).
[34]J. Nagle, Faraday Discuss. **161**, 11 (2013).
[35]B. Jojart and T. A. Martinek, J. Comput. Chem. **28**, 2051 (2007).
[36]L. Janosi and A. Gorfe, J. Chem. Theory Comput. **6**, 3267 (2010).
[37]D. Poger and A. Mark, J. Chem. Theory Comput. **6**, 325 (2010).
[38]D. Boal, *Mechanics of the Cell* (Cambridge University Press, Cambridge, 2002).
[39]W. Rawicz, K. C. Olbrich, T. McIntosh, D. Needham, and E. Evans, Biophys. J. **79**, 328 (2000).
[40]E. Evans and W. Rawicz, Phys. Rev. Lett. **64**, 2094 (1990).
[41]H. Binder and K. Gawrisch, J. Phys. Chem. B **105**, 12378 (2001).
[42]J. F. Nagle, M. S. Jablin, S. Tristram-Nagle, and K. Akabori, Chem. Phys. Lipids **185**, 3 (2015).